Topographic optical profilometry by absorption in liquids

Juan Carlos Martinez Antón,[1,*] Jose Alonso,[1] Jose Antonio Gómez Pedrero,[1] and Juan Antonio Quiroga[2]

[1]*Departamento de Óptica, Escuela Universitaria de Óptica, Universidad Complutense de Madrid, C/. Arcos de Jalón 118, 28037, Madrid, Spain*

[2]*Departamento de Óptica, Facultad de Ciencias Físicas, Universidad Complutense de Madrid, Ciudad Universitaria s/n, 28040, Madrid, Spain*

[*]*jcmartin@fis.ucm.es*

Abstract: Optical absorbance within a liquid is used as a photometric probe to measure the topography of optical surfaces relative to a reference. The liquid fills the gap between the reference surface and the measuring surface. By comparing two transmission images at different wavelengths we can profile the height distribution in a simple and reliable way. The presented method handles steep surface slopes (<90°) without difficulty. It adapts well to any field of view and height range (peak to valley). A height resolution in the order of the nanometer may be achieved and the height range can be tailored by adapting the concentration of water soluble dyes. It is especially appropriate for 3D profiling of transparent complex optical surfaces, like those found in micro-optic arrays and for Fresnel, aspheric or free-form lenses, which are very difficult to measure by other optical methods. We show some experimental results to validate its capabilities as a metrological tool and handling of steep surface slopes.

OCIS codes: (120.0120) Instrumentation, measurement, and metrology; (120.6650) Surface measurements, figure; (120.4630) Optical inspection; (110.4155) Multiframe image processing; (220.1250) Aspherics; (230.3990) Micro-optical devices.

References and links

1. K. P. Thompson and J. P. Rolland, "A revolution in imaging optical design," Opt. Photon. News **23**(6), 30–35 (2012).
2. C. C. Lai and I. J. Hsu, "Surface profilometry with composite interferometer," Opt. Express **15**(21), 13949–13956 (2007).
3. L. Deck and P. de Groot, "High-speed noncontact profiler based on scanning white-light interferometry," Appl. Opt. **33**(31), 7334–7338 (1994).
4. J. C. Wyant, "Advances in interferometric surface measurement," Proc. SPIE **6024**, 602401, 602401-11 (2006).
5. C. Zhao, J. Tan, J. Tang, T. Liu, and J. Liu, "Confocal simultaneous phase-shifting interferometry," Appl. Opt. **50**(5), 655–661 (2011).
6. C. H. Lee, H. Y. Mong, and W. C. Lin, "Noninterferometric wide-field optical profilometry with nanometer depth resolution," Opt. Lett. **27**(20), 1773–1775 (2002).
7. F. Blais, "Review of 20 years of range sensor development," J. Electron. Imaging **13**(1), 231–243 (2004).
8. F. Chen, G. M. Brown, and M. Song, "Overview of three-dimensional shape measurement using optical methods," Opt. Eng. **39**(1), 10–22 (2000).
9. D. Purcell, A. Suratkar, A. Davies, F. Farahi, H. Ottevaere, and H. Thienpont, "Interferometric technique for faceted microstructure metrology using an index matching liquid," Appl. Opt. **49**(4), 732–738 (2010).
10. G. Svensson, "A method for measurement of the absorption in extremely high-absorbing solutions," Exp. Cell Res. **9**(3), 428–433 (1955).
11. M. Csete and Z. Bor, "Plano-concave microcuvette for measuring the absorption coefficient of highly absorbing liquids," Appl. Opt. **36**(10), 2133–2138 (1997).
12. J. Johnson and T. Harris, "Full-field optical thickness profilometry of semitransparent thin films with transmission densitometry," Appl. Opt. **49**(15), 2920–2928 (2010).
13. S. Ogilvie, E. Isakov, C. Taylor, and P. Glover, "A new high resolution optical method for obtaining the topography of fracture surfaces in rocks," Image Anal. Stereol. **21**(1), 61–66 (2002).
14. E. Isakov, S. R. Ogilvie, C. W. Taylor, and P. W. J. Glover, "Fluid flow through rough fractures in rocks 1: high resolution aperture determinations," Earth Planet. Sci. Lett. **191**(3-4), 267–282 (2001).

#177047 - $15.00 USD Received 27 Sep 2012; revised 11 Nov 2012; accepted 18 Nov 2012; published 10 Dec 2012

15. M. A. Model, A. K. Khitrin, and J. L. Blank, "Measurement of the absorption of concentrated dyes and their use for quantitative imaging of surface topography," J. Microsc. **231**(1), 156–167 (2008).
16. J. C. Martínez Antón, J. A. Gómez Pedrero, J. Alonso Fernández, and J. A. Quiroga, "Optical method for the surface topographic characterization of Fresnel lenses," Proc. SPIE **8169**, 816910-8 (2011).

1. Introduction

Profilometry of optical surfaces is of increasing importance and difficulty as optical devices expand its applications and surface topologies are more complex, like in Fresnel optics, micro-optical arrays, free-form lenses [1], etc… There are numerous non-contact optical methods to determine the topography of surfaces. Most of them use the reflection of light on the surface to be measured and they are mainly based on interferometry [2–4], confocal profilometry [5,6] and structured light projection and triangulation techniques [7,8]. However, for most conventional approaches, a high surface slope is difficult to handle. Different aspects are behind this fact, being the more basic that the light is lost when reflection occurs at high surface slopes.

In this work, we propose an optical profilometric method that works with transmitted light and is based on the optical absorption in a dye solution, which codifies height variations. The use of transmitted light through liquids is interesting for the optical determination of surface topography [9–15]. In the work of Purcell *et al* [9] a non-absorbing liquid is used to reduce the apparent surface slope by index matching with the surface materials and therefore controlling refraction. This allows the use of known interference techniques to explore micro-prisms and other steep surface profiles successfully [9]. On the other hand, the use of optical absorption to estimate depth or thickness is not new [10–15]. Although the Lambert-Beer law is commonly used to calculate the specific absorption of substances [10,11], it can be seen the other way around, i.e., used to estimate the thickness of solid films [12], or more interesting to our goal, to obtain the relative profile of a surface compared to a reference surface when a liquid with known absorption fills the space between both elements [13–15]. To apply this last strategy correctly a reference optical signal is necessary. In the work of Ogilvie *et al* [13,14] this is accomplished by using clear water instead of the dye solution in the same setup. This approach is cumbersome and the procedure is prone to misalignment and other errors like dye contamination. Model *et al* [15] work under the assumption of constant irradiance over the surface. But in their setup, the aperture limited illumination may lead to profile errors particularly for very steep surfaces, where again, light may be lost by refraction.

We introduce two improvements in the topographic optical profilometry by absorption in fluids which lead to a greater reliability of the technique. First, we use two narrow spectral bands for illuminating. In this way, we get an absorption signal and a reference signal without moving any component in the setup. Furthermore, a constant ratio between the radiances of both spectral bands guarantees a non-distorted profile measurement. Secondly, we use extended light sources to reach high numerical apertures of illumination. This strategy allows measuring steep slopes (<90°) in a simple way.

In a previous work [16] we used LED sources, but a calibration procedure is then necessary.. Now, we introduce monochromatic laser sources which intrinsically provide a linear model, simplifying, in this way, the experimental procedure and data analysis. Several measurements are shown here to demonstrate good metrological properties of the technique in terms of reproducibility and resolution. We achieve a height resolution in the order of nanometers, comparing favorably with other known techniques, but with the added advantage of handling steep slopes without difficulty.

2. Description of the method

A reference surface is located close to the surface we want to profile (Fig. 1). An optical absorbing liquid or fluid fills the gap between the surface to measure and a reference surface. This optical sandwich is situated between an extended light source and an imaging device focused at the surface to profile. Images are captured for different spectral bands. The differential absorption between these bands provides direct information of the surface

#177047 - $15.00 USD Received 27 Sep 2012; revised 11 Nov 2012; accepted 18 Nov 2012; published 10 Dec 2012

topography. The basic procedure consists on taking images at two narrow spectral bands centered at λ_A and λ_R. They are selected so that the absorption of the dye is significantly greater at λ_A, and the band centered at λ_R is used to provide a reference signal.

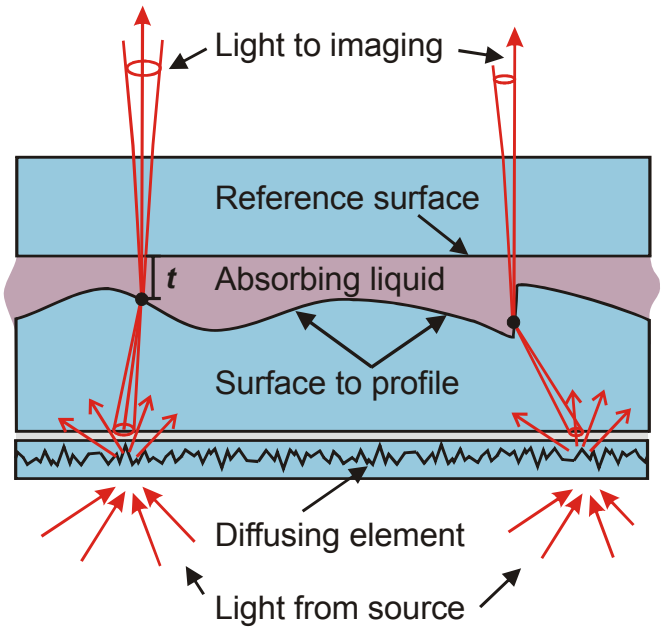

Fig. 1. Basic configuration for the sample to be measured.

An extended light source provides wide spread angular illumination (for example an integrating sphere). Also, a diffusing element optically coupled may also be used to increase the illuminating angular aperture at the surface to profile (Fig. 1). In this way, at every point of the surface to profile, we make sure that the light beams will reach the entrance pupil of the imaging device, independently of ray refraction at slopes.

We will adopt several assumptions to simplify the formal analysis: 1) the optical surface to analyze and a reference surface are part of transparent substrates with constant transmittance over the explored area. 2) The imaging system captures a thin light beam from every imaged point. 3) The fluid has a refractive index close to optically match at least one of the surfaces (reference or sample) in order to neglect multiple reflections and take into account a single pass. 4) We will consider that the reference surface belongs to a glass plate with parallel surfaces as illustrated in Fig. 1. 5) The imaging system is telecentric or, in other words, the probe beams are perpendicular to the reference surface plane. This last condition allows the surface profile to be expressed as a height related to this reference plane (Fig. 1).

There are several ways to measure the transmittance within the liquid which is the basis for the profilometric probe. We describe here our preferred procedure because its simplicity and robustness. The imaging system provides an image proportional to the transmitted radiance L of the sample that can be expressed as (Lambert-Beer law)

$$L = L_0 T \exp(-\alpha \cdot t), \tag{1}$$

where L_0 is the radiance of the extended light source taken at the considered surface point and line of sight (beam trajectory), T is the total transmittance of the measuring plate-reference plate system except for the internal liquid transmittance that is included in the exponential term, where α is the absorption coefficient of the liquid and t is the distance from a reference surface point to a sample surface point as shown in Fig. 1 (consider it positive).

Consider now that the extended light source of Fig. 1 provides illumination at two different narrow spectral bands, centered at wavelengths λ_R and λ_A. The absorption

#177047 - $15.00 USD Received 27 Sep 2012; revised 11 Nov 2012; accepted 18 Nov 2012; published 10 Dec 2012

coefficients of the liquid for these wavelengths are α_R and α_A respectively (see Fig. 2). We define the measuring magnitude M as the ratio of two images taken at these two illuminations, pixel by pixel, i.e.:

$$M = \frac{L_{0A}T_A \exp(-\alpha_A \cdot t)}{L_{0R}T_R \exp(-\alpha_R \cdot t)} = C \exp\left[-(\alpha_A - \alpha_R)\cdot t\right], \tag{2}$$

where C ($C = L_{0A}T_A/L_{0R}T_R$) is a system factor that does not depend on the profile. This system parameter C should be a constant. For uniform transmittances at reference and sample substrates the ratio T_A/T_R is a constant. Furthermore, the ratio L_{0A}/L_{0R} is constant for Lambertian light sources like integrating spheres, but not only. In fact, a spatially non-uniform light source could be used if the ratio between radiances at the reference and absorbing spectral bands is constant. In other words, light from the illuminating source may be spatially non-uniform but it has to be chromatically constant (same color independently of point and angle of observation). We may rewrite expression (2) as

$$M = \exp\left[-\alpha_S (t - t_0)\right], \tag{3}$$

where $\alpha_S = \alpha_A - \alpha_R$, and t_0 comes from rewriting C as $C = \exp(\alpha_S\, t_0)$. Finally, we can calculate the profile point by point from Eq. (3) by using the following form:

$$t = t_0 - \ln(M)\cdot t_S, \tag{4}$$

where the characteristic distance t_S is related to the differential absorption α_S as $t_S = 1/\alpha_S$. The parameter t_0 represents a baseline height or piston surface that is constant.

The characteristic parameter t_S can be seen as synthetic skin depth and basically defines the height range of the method. For the particular case of zero absorption at the reference wavelength (λ_R), the parameter t_S represents the distance that the light at absorbing wavelength (λ_A) propagates within the liquid just to be attenuated to ~37% (T = 1/e). As it depends on absorption, it can be set to different values simply by varying the concentration of a soluble dye. As we see next, both the achievable height resolution and the height range are linked to t_S in a fundamental way.

The expected height sensitivity (Δt) can be estimated from Eq. (4) as

$$\Delta t = -(\Delta M/M)\cdot t_S, \tag{5}$$

which conveniently express a small height variation Δt in terms of a small relative variation of the measured ratio ($\Delta M/M$) and the characteristic distance of the absorbing fluid t_S. Considering now this variation as an uncertainty coming from a random process, we may see Δt in Eq. (5) as the ultimate resolution of a measurement. This depends basically on the signal to noise ratio (SNR) of the imaging device. Signal to noise ratio can be defined as SNR = $N/\Delta N$ where N is the signal reading at CCD (expressed in digitizer counts N) and proportional to radiance L and ΔN is the final noise. For a scientific CCD camera working near the saturation level, SNR can be typically estimated as the square root of the electron well depth. Typical values for the SNR of a single pixel are between 40:1 and 120:1. Usually we take a maximum of 4 different images (with the background subtracted), a minimum of 2 of them for the estimation of the absorption and reference and other 2 for calibration of the photo-response non-uniformity (PRNU) of the CCD. This calibration is necessary to make the piston term t_0 really a constant and not dependent on a non-uniform response of the CCD. A four image processing leads to a final uncertainty in magnitude M of $\Delta M/M$ = 2/SNR, i.e. the best height resolution Δt is about a ~2% of t_S in a single shot acquisition and per pixel. Multiple frame integration and/or spatial pixel averaging can increase SNR and therefore height resolution in one or two orders of magnitude as we will see in the experimental results. Therefore, in general terms, a final height resolution better than $10^{-3}t_S$ can be reasonably expected. On the other hand, we may find highly absorbing substances with t_S values even

#177047 - $15.00 USD Received 27 Sep 2012; revised 11 Nov 2012; accepted 18 Nov 2012; published 10 Dec 2012

below 1 micron for concentrated solutions. According to our previous analysis this means that nanometer-level height resolution is achievable.

The photometric dynamic range of the imaging capturing device determines the height profile range (peak to valley) of the method. In practice, the height range is not much bigger than t_S because of the exponential decay of transmission. For example, at a depth of $4t_S$ the transmittance is reduced to a mere ~2%. We may increase the height range by one order of magnitude and still preserving the height resolution by using high dynamic range imaging (HDRI techniques) which is equivalent to expand the photometric range of the imaging device. Notice that both height resolution and height dynamic range are linked to the fluid parameter t_S and this parameter can be adapted by means of changing the dye concentration.

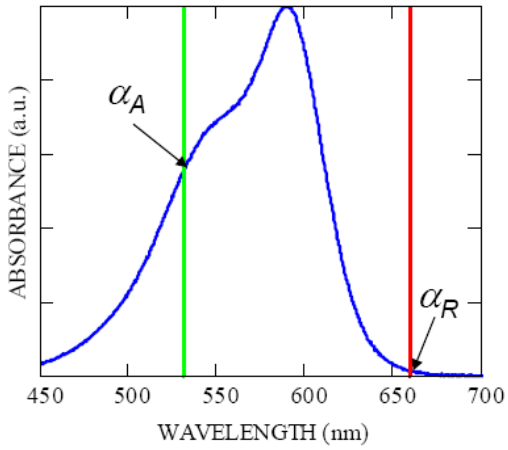

Fig. 2. Absorption spectra of methyl violet dye in water (blue line) and the laser lines used for reference (red) and for sampling (green) in the measurements.

3. Experimental results

We implemented a set-up similar to Fig. 1 with an integrating sphere as extended uniform light source. The integrating sphere was illuminated with two diode laser beams, one at λ_A = 532 nm and the other at λ_R = 660 nm through the same input port. In a previous paper [15] the primary light sources were LEDs. The LEDs are simple to operate and cheap, but they make difficult the use of the technique as a metrological tool. The reason is that most dyes have a variable absorption over the LED spectrum. Because of this, thickness estimation does not depend linearly with ln(M), as stated in Eq. (4), and a careful calibration of the nonlinear relationship must be done for any dye-LED combination. Monochromatic laser sources do not have this problem, but they lead to a great amount of speckle noise. To average speckle noise out, we have used random pointing of the laser beam with an electromechanical oscillating device (white noise fed) fitted to the laser body. Both lasers are aimed at the same central point within the integrating sphere to guarantee a constant radiance ratio at the exit port between both light sources.

As a basic absorbing fluid we used a saturated solution of methyl violet dye (CAS#8004-87-3) in a mixture of water (13.5% by weight) and glycerol (86.5%) and filtered to 0.8 μm particles. The glycerol-water mixture has proven adequate to avoid evaporation/condensation of water that would change absorption properties. The ambient at the lab were typically at T = 25 ± 2°C and at a relative humidity of 51 ± 3% measured with a Brannan type hygrometer. The absorption spectrum of the liquid and the wavelengths of illumination are shown in Fig. 2. Under these conditions the fluid is found to have a t_S of 6.63 ± 0.05 μm, obtained from a method we will explain later.

The digital imaging capturing device was a CCD array of 1340x1024 pixels (model ORCA C4742-96-12G04) with a well depth of 18000 electrons and a 12 bit signal digitizer.

#177047 - $15.00 USD Received 27 Sep 2012; revised 11 Nov 2012; accepted 18 Nov 2012; published 10 Dec 2012

Operation was typically made between 5% and 40% of the saturation level to be sure that a deviation from linearity of the response is below 0.1%. At 40% signal level the SNR is about 80:1. A zoom lens was used to focus images on the CCD in a quasi-telecentric mode (model NT58-240 from Edmund Optics). Spatial photo-detector response non uniformity (PNRU) was also characterized by taking images of uniform irradiance coming directly from the integrating sphere at both wavelengths λ_A and λ_R. These images are used to correct the effect of PRNU. We insert in Eq. (4) the magnitude M estimated as $M = M_m/M_p$ where M_p is the ratio of images of direct observation of extended light source at both wavelengths $M_p = R_A/R_R$ (R signal at the CCD) and M_m is the equivalent ratio but with the sample-reference setup in the optical path. A maximum signal to noise ratio SNR of ~900:1 is obtained when 128 frame averaging is performed for a single image capture.

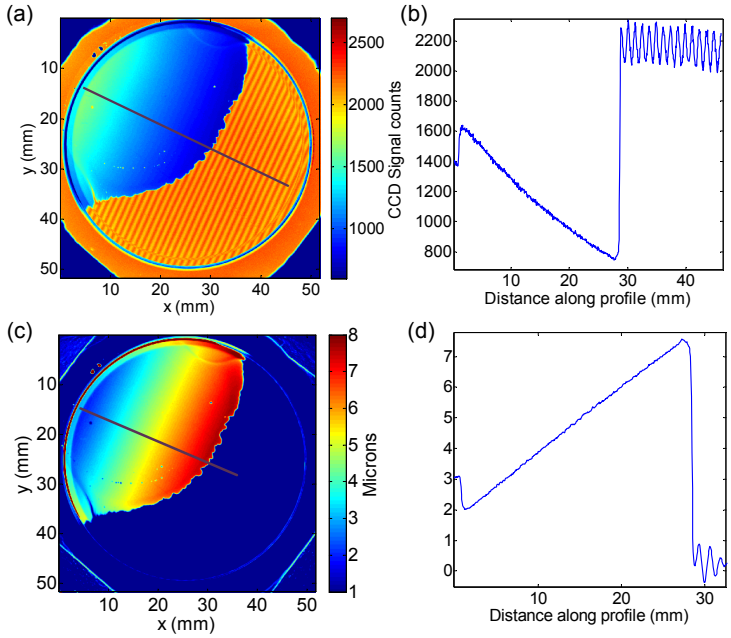

Fig. 3. (a) Image of a thin wedge between flats and partially filled with absorbing fluid. Interference fringes are observed at the air gap. (b) Signal profile along the line drawn in (a). Notice the exponential decay in the absorption region and the fringe contrast in the air gap side. (c) Topographic image of the wedge of by processing the image of (a) applying Eq. (4). (d) Height profile along the line drawn in (c), ordinate axis is in microns.

A first test was performed to validate Eq. (4) and the experimental setup and also served to obtain the parameter t_S of the prepared absorption solution. Two flats were arranged to make a very thin wedge prism, partially filled with the absorber and partially filled with air. One flat is λ/20 and the other is λ/10. Under the illumination setup described we obtain the image in Fig. 3(a). There we find a variable absorption area corresponding to the region of the prismatic gap filled with the liquid, and also a fringe interference pattern in the other side. In the fringed interference region we make a simple calculation of thickness slope perpendicular to the fringes. Each fringe corresponds with a λ/2 height increment (= 266 nm). From the interference fringe analysis we obtain a wedge slope of $\Delta t/\Delta x = (2.16 \pm 0.01)\cdot 10^{-4}$, which represents a height variation of 0.216 μm per millimeter of length perpendicular to the fringe pattern. In the absorbing side we can obtain the maximum slope of ln(M) which we know is proportional to the height variation. The proportionality constant is the absorption parameter t_S (Eq. (4)). The comparison with the interference data get the result of $t_S = 6.63 \pm 0.05$ μm.

#177047 - $15.00 USD Received 27 Sep 2012; revised 11 Nov 2012; accepted 18 Nov 2012; published 10 Dec 2012

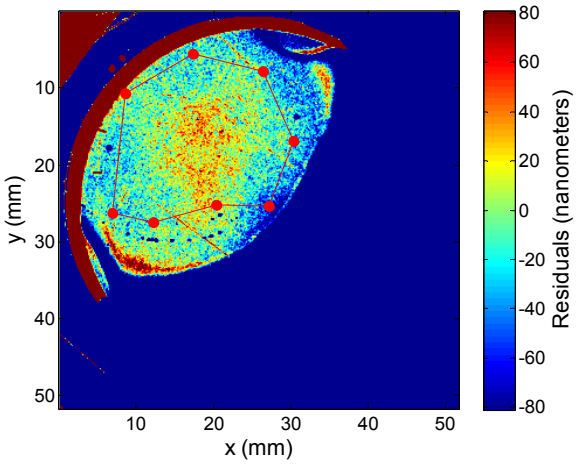

Fig. 4. Residuals of a regression fit to a plane for the image of Fig. 4. Regression is only computed within the red polygon drawn.

Applying Eq. (4) with the estimated t_S we obtain the results shown in Fig. 3(d). We may appreciate a linear thickness profile as was expected from a wedge. A more exigent data processing is shown in Fig. 4 where we show the residuals of a regression fit to a plane for the ln(*M*) image. A region of interest (red polygon in the figure) was selected for the regression in order to avoid bubbles that may distort the result. We obtain a RMS form deviation of ± 22 nm and a peak to valley deviation of ~65 nm which is in agreement with the nominal data of the surfaces, a λ/10 flat on a λ/20 flat (or an equivalent peak to valley deviation of 90 nm at worst). Some diagonal nearly parallel lines are observed crossing the field of view. After cleaning and observing the sample flat under intense illumination, scattered light confirmed the presence of slight scratches that explain this feature. In the Fig. 4 we may also appreciate on the left and on top some curved strips that are probably due to residual humidity in the flat surface coming from a preliminary wet cleaning. This humidity residue changes locally the absorption of the liquid and provokes these artifacts.

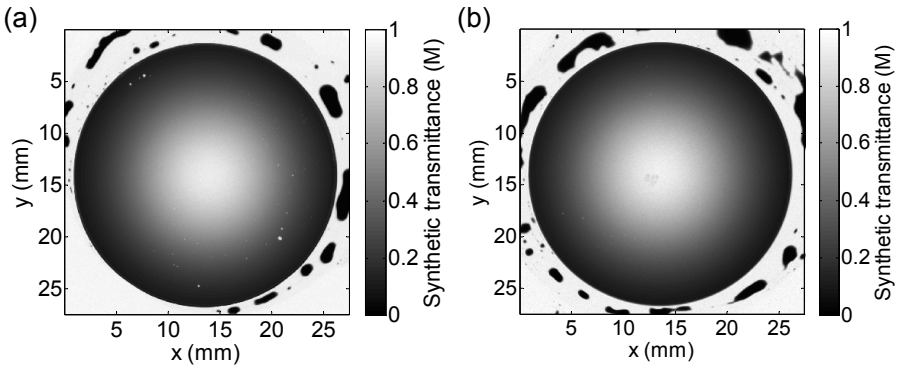

Fig. 5. Images of the synthetic transmittance *M* of a plano-convex lens: (a) measurement in day 1 and (b) after 5 days and rotating and displacing the lens to test reproducibility.

A second topographic measurement was performed on a spherical surface compared against a flat surface as a reference. The sphere comes from a 1" aperture BK7 plano-convex lens (model PLCX-25.4-5151.0-C from CVI Melles Griot corp.) with a nominal radius of R = 5151 ± 26mm. The surface accuracy is stated as λ/10 (~60 nm) over the 85% of the aperture. The reference surface is a λ/20 silica flat with an aperture of 3". The convex surface was lying down on the flat with the absorption liquid in between. Viscosity and surface tension keep the

#177047 - $15.00 USD Received 27 Sep 2012; revised 11 Nov 2012; accepted 18 Nov 2012; published 10 Dec 2012

fluid in place. The other face of the flat was index matched to a diffusing opal glass and finally the stack of the three glass pieces is laid down on the exit port of the illuminating integrating sphere (~2.5" aperture).

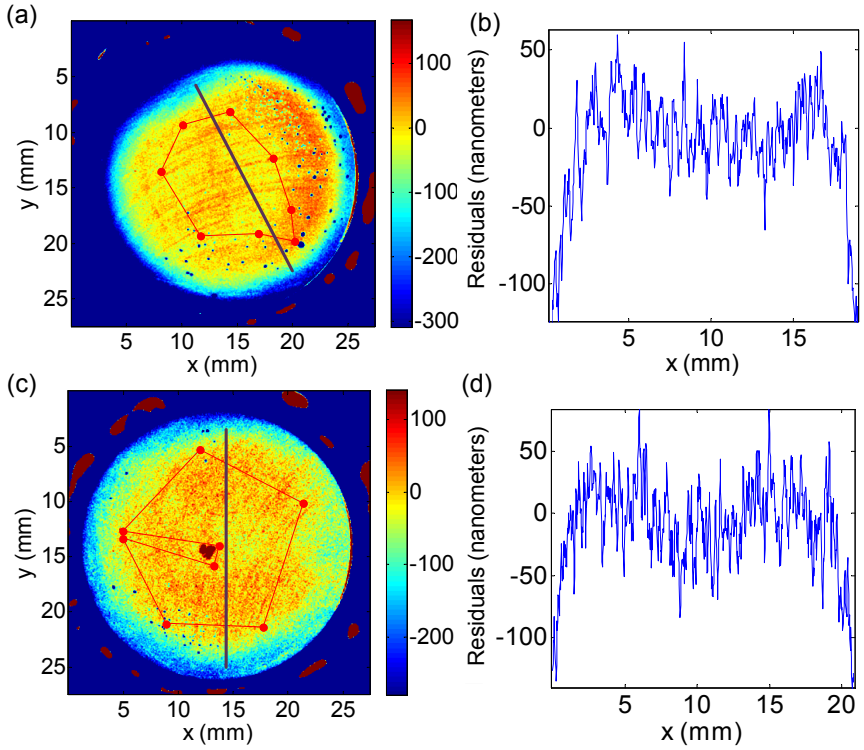

Fig. 6. Results on the spherical surface of a spherical lens (R = 5151mm). (a) Regression fit residuals of the processed measurements of Fig. 5(a). (b) the same as (a) but for Fig. 5(b). (b) and (d) are linear profiles of fit residuals along the lines drawn in (a) and (c) respectively.

Several measurements of the lens were performed on different days. In the mean time, the lens was rotated and displaced to extract some bubbles but keeping the same absorbing liquid and exposed to the open air. This was done to check reproducibility of measurements against evaporation/condensation and manipulation. For each measurement we take two images (at λ_A and λ_R) with background removed and correct them with PRNU images to get the processed image *M*. By means of Eq. (4) we obtain topographic images like the ones shown in Fig. 5 for day 1 and day 5. For each topographic image we make a regression fit to an ideal spherical surface. What it is shown at Fig. 6 are the residuals of the regression fit for days 1 and 5. The regression is performed in a selected region (red polygon drawn in Fig. 6(a) and 6(c)) avoiding the presence of bubbles.

For the estimation of the radius of the sphere we need the length scale of the image and this was obtained from the known size of the lens (25.3 ± 0.05 mm). We also assumed no appreciable imaging distortion in the regression area. The method finally provides good results, matching the expectations. From 5 different measurements we obtain an averaged radius of curvature of R = 5170 ± 60mm which agrees with the nominal data of R = 5151 ± 26mm. Possible time-shifts or evaporation effects are included in the uncertainty but are practically unappreciable. The RMS form deviation for each regression fit is around ~ ± 27 nm which is in agreement with the nominal figure of merit for a λ/10 surface. Height resolution according to Eq. (5) is expected to be around ~ ± 15 nm, which is consistent with the observed residuals in Fig. 6(b) and 6(d). Finally, appreciable deviations of residuals are

#177047 - $15.00 USD Received 27 Sep 2012; revised 11 Nov 2012; accepted 18 Nov 2012; published 10 Dec 2012

observed at the rim of the lens but these are still consistent with being a nominal λ/10 surface only over the 85% of the aperture.

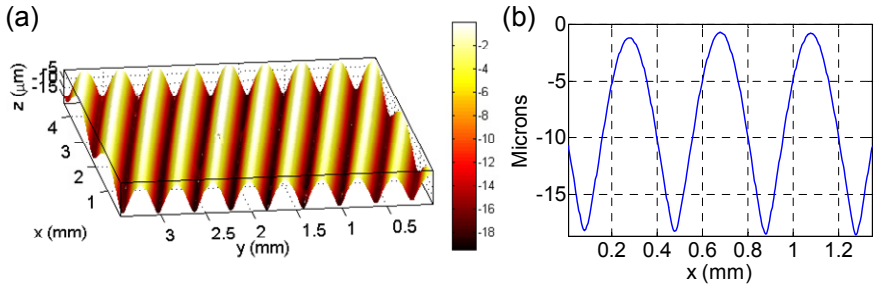

Fig. 7. Topography of a cylindrical lens array. (a) 3D rendering of a profilometric measurement. (b) Partial linear profile along a line perpendicular to the array axis.

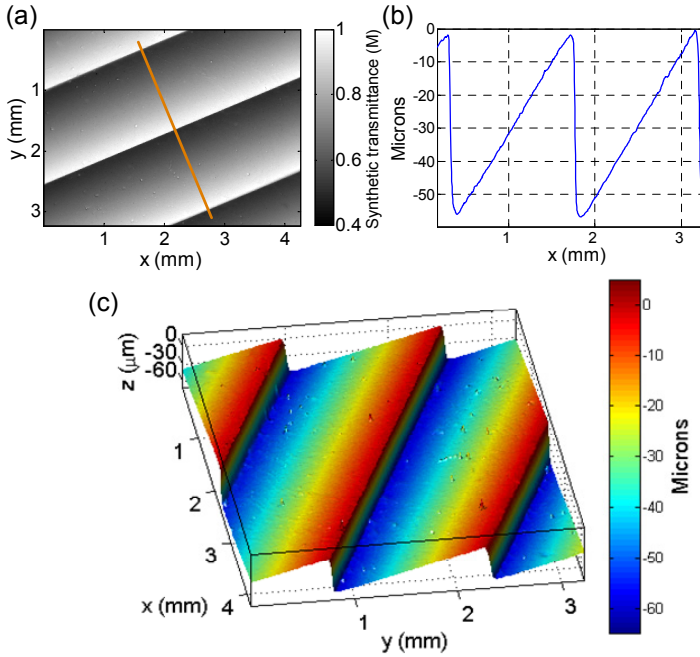

Fig. 8. Prismatic array. (a) image ratio *M*, (b) partial height profile perpendicular to prism edges (c) 3D representation of the full field of view.

Although the former tests demonstrate the capabilities of the method as a reliable metrological tool, perhaps it does not add special value to measure spheres, mild aspheres or flats, for which standard interferometric tools are well established and recognized. On the contrary, the method may stand out for measuring complicated shapes and high slopes on macro and micro optical components and arrays. For them, the method still provides speed, height resolution and accuracy with a simple and robust experimental procedure.

For example, Fig. 7 shows the results for a cylindrical micro-lens array of 64 lenses per inch and nominal sag of 18 μm in quite agreement with extracted profile (Fig. 7(b)). In another example, we show in Fig. 8 the measurement of a micro-prism linear array used in eye care. It has a peak to valley height of 57 μm and a period of 1.43 mm. Absorption solution in this case was diluted to have t_S = 85 μm. A maximum nominal slope of 90° is expected at the edges of the prisms. In practice, we find in the measurement that the abrupt

#177047 - $15.00 USD Received 27 Sep 2012; revised 11 Nov 2012; accepted 18 Nov 2012; published 10 Dec 2012

height change is handled without difficulty, although somewhat smoothed due to the lateral imaging resolution (Fig. 8). Finally, we show in Fig. 9 the results for a measured linear array or prisms with facets symmetrically arranged at an angle of 60°, and at a period of 0.64 mm (Fresnel Technologies part#420). For this sample we use a dye solution with t_S = 754 μm. The results shown in the linear profiles are in good agreement with the nominal values expected for all the arrays. Some particles contamination is noticeable in the case of the prism array of Fig. 8 and also bubbles are usually present in all measurements. They behave as blind spots but do not affect the processing of information of nearby areas because Eq. (4) is applied for every single pixel independently of the neighbors.

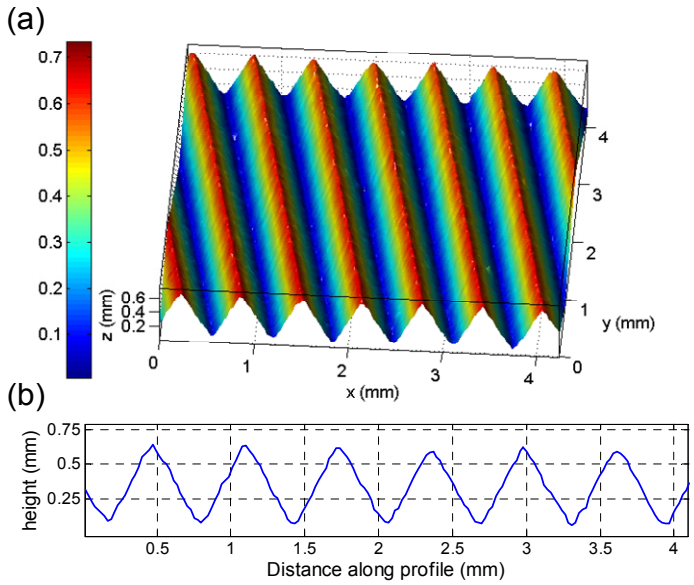

Fig. 9. Linear array of prisms (apex of 60°). (a) 3D rendering of processed image ratio *M*, (b) height profile along a line perpendicular to prism wedges. Notice the horizontal and vertical scales are the same in both representations.

5. Conclusions

We demonstrate the feasibility of topographic optical profilometry by absorption in liquids. The method is especially appropriate for all type of transmission optical devices with complex surface forms and patterns. Height resolution and form accuracy in the order of the nanometer has been achieved. The method can handle steep surface slopes in contrast to other know reflection based techniques. We may point out also other features: 1) it is simple to implement with no-moving parts in contrast to confocal and/or interferometric profilometers and 2) it can be fast besides some sample preparation that is required.

Acknowledgments

This work has been developed within the framework of the project DPI2009-09023 financially supported by Spanish MICINN (Ministerio de Ciencia e Innovación).